12th International Conference on Structural Analysis of Historical Constructions
SAHC 2020
P. Roca, L. Pelà and C. Molins (Eds.)

COMBINED SHEAR-FLEXURAL VERIFICATION OF IN PLANE LOADED REINFORCED AND UNREINFORCED MASONRY WALLS

ANDREA BENEDETTI[*1], MIRCO TAROZZI[1] AND LORENZO BENEDETTI[2]

[1]DICAM Department
Università degli Studi di Bologna
2, Viale Risorgimento, 40136 Bologna, Italy
e-mail: andrea.benedetti@unibo.it, www.unibo.it/en (*corresponding author)

[2]STI DESL, Ecole Polytechnique Fédéral Lausanne
ELL 166 Station 11
CH-1015 Lausanne, Switzerland
Web page: https://people.epfl.ch/lorenzo.benedetti?lang=en

Keywords: Masonry panel, in-plane loading, shear-flexural verification, reinforcement design

Abstract. *The safety verification of in-plane loaded masonry panels requires the evaluation of at least three different collapse conditions connected with overturning, shear sliding, and shear – compression failure at the panels' toe. In reinforced panels, the resisting models should even take into consideration the presence of localized or distributed reinforcement.*

In general, the masonry is considered a Mohr-Coulomb type material not resisting tension and plastic in compression, while reinforcement is a brittle elastic material resisting tensile forces only [1].

The ultimate limit state is however linked with a given subset of compressed material inside the panel area. The compressed sections are therefore varying inside the panel as a function of the applied load. The collapse occurs in shear or overturning when one peculiar compressed section reduces to its minimum [2].

By equating the capacity in shear and overturning it is possible to derive an explicit statement of the minimum length of the compressed section which will be activated by a simultaneous failure in shear and overturning. A simple inequality is detecting the real failure mode and this allows directly computing the failure load resultant.

The procedure is very fast and can deal even with localized or distributed reinforcement layers such as fiber strips or mesh reinforced mortars.

Some examples of panels discussed in the literature show the effectiveness of the proposed verification procedure.

1 INTRODUCTION

As is well-known masonry panels under in-plane loading can exhibit several collapse forms according to the combination of geometry, restraint, axial and shear forces acting on it.

In particular, due to the low tensile capacity of masonry materials, small axial compression forces lead to moderate shear capacities, mainly linked to the cohesion of the material.

If the horizontal displacement demand increases, cracks running on the mortar joints will appear in the masonry panel, reducing thus the length of the compressed zone along the height of the panel. In the cracked condition, the shear is carried on by the compressed area only, producing so a mixed compression-shear state on the masonry. At the shear peak value, the panel can collapse alternately with rocking failure until overturning, or with sliding failure with progressive crack opening.

Collapse by overturning is typical of slender panels under low or moderate axial forces, while shear sliding is typical of very squat walls. When the axial force is very high or the compressive masonry strength is very low, the probability that the panel will fail with shear crushing of the compressed toe increases considerably. In this case, inclined diagonal cracks splitting the bricks arise on the panels.

In this paper, the problem of mixed shear-rocking failure is solved by determining the compressed zone length that makes the shear producing overturning and sliding the same. A closed formula allows computing the ending geometry of stable behavior. Namely, after this point, by decreasing the size of the compressed zone even the shear has to reduce its value in a softening branch. The limit value that results in a shear-crushing of the toe is even expressed in terms of the Mohr-Coulomb failure criterion.

In order to validate the analytical formulation, several experimental campaigns presented in the literature takes as a reference and their findings are discussed in the following.

2 COMBINED SHEAR – FLEXURAL FAILURE OF MASONRY PANELS

Considering a rectangular panel of constant thickness t_M acted on by a linear bending moment distribution it is in any case possible to extract a cantilever part of it which can be considered the part relevant for the failure. The height of this cantilever is given by the ratio of the largest bending moment M_S to the shear force V_S and is equivalent to a shear arm a_V:

$$a_V = \frac{M_S}{V_S} \tag{1}$$

As a consequence of the limited tensile resistance of the masonry texture and beyond a certain shear force, the base section of the cantilever begins to crack, and therefore the equilibrium is guaranteed by the eccentricity of the stress resultant acting on the contact area.

The verification of this incipient failure situation is in general carried out by using different formulas for the possible collapse modes: flexural overturning, shear sliding and shear-compression crushing (according to the Mohr-Coulomb criterion, see [1]).

$$V_{R,fl} = \frac{N_S L}{2a_V}\left(1 - \frac{N_S}{\kappa N_P}\right) \tag{2.a}$$

$$V_{R,sh} = \mu N_S + \beta t_M \, f_{MV0} \tag{2.b}$$

$$V_{R,MC} = \beta t_M \, f_{MV0} \sqrt{\left(1+\frac{\sigma_0}{f_{Mt}}\right)\cdot\left(1-\frac{\sigma_0}{f_{Mc}}\right)} \tag{2.c}$$

In the given formulas N_S is the axial force in the panel, L and t are the length and the thickness of the panel' section, f_{Mc} and f_{Mt} are respectively the compressive and tensile strength of the masonry material, β is the length of the compressed area in the base section, κ and μ are the ductility and friction coefficients. The other variables are as follows:

$$N_P = L t_M \, f_{Mc} \quad , \quad f_{MV0} = \frac{f_{Mt}\cdot f_{Mc}}{f_{Mt}+f_{Mc}} \quad , \quad \sigma_0 = \frac{N_S}{\beta t_M} \, . \tag{3}$$

It is to note that the shear-compression failure formula derived in agreement with the Mohr-Coulomb criterion is very similar to the Turnsek-Cacovic formula if the axial stress is not very high:

$$\tau_{R,MC} = \tau_{R,TC} \cdot \sqrt{\left(1-\frac{\sigma_0}{f_{Mc}}\right)} \tag{4}$$

The resisting shear stress is obviously the minimum among the three formulas (2).

Since masonry in compression can be considered an elastic perfectly plastic material [3], the stress distribution at the panel's base is a consequence of the linear strain distribution. By assuming that the ductility D of the material is described by the ratio of the ultimate strain ε_{ult} to the limit elastic one ε_e, the resultant of the stress distribution can be expressed in terms of the compressed area and the ductility ratio D.

If the cantilever is very slender, the failure is occurring by overturning with the minimal length of the contact area:

$$\beta_{\min} = \frac{2D}{2D-1}\cdot\frac{N_S}{t_M \, f_{Mc}} \tag{5}$$

If the cantilever is sufficiently squat, the failure is occurring by shear with a compressed zone larger than the minimal one. The value of the compressed length at failure can be computed by equating the shear force producing sliding with the one producing overturning:

$$\frac{M_{R,fl}}{a_V} = \frac{N_S}{a_V}\left(\frac{L}{2}-\frac{\bar{\beta}}{n}\right) = \mu N_S + \bar{\beta}\, t_M \, f_{MV0} = V_{R,sh} \tag{6.a}$$

$$\beta_{\lim} = \bar{\beta} = \frac{n}{2}\,\frac{N_S\left(L-2\mu\, a_V\right)}{N_S + n\, a_V \, t_M \, f_{MV0}} \geq \beta_{\min} \tag{6.b}$$

The value of the parameter n is defining the adimensional distance of the stress resultant force from the edge of the panel:

$$n = \frac{1+3D\left(D-1\right)}{3D\left(2D-1\right)} \tag{7}$$

Since the deflection of the cantilever can only increase if the shear is increasing and the compressed length is decreasing (in order to guarantee the rotational equilibrium), the limit $\bar{\beta}$ defines even the limit stable displacement of the panel. If the shear - displacement curve of the panel is known, the curve must be cut at $V_{R,\lim}$ given by $\beta_{\lim}$.

Many procedures exist that can allow plotting the shear - displacement curve up to panel overturning (see among the others [4, 5]). One very simple procedure allowing for well-approximated shear displacement curves is the use of hyperbolic functions. As is usual in geotechnics, only two parameters are necessary to build up an effective relationship:

$$V(\delta) = \delta \cdot \left(\frac{1}{K_0} + \frac{\delta}{V_{\lim}} \right)^{-1} \tag{8}$$

In which K_0 is the initial stiffness of the panel and $V_{\lim}$ the maximum resisting shear when the displacement tends toward infinity.

If masonry panels are concern, the initial stiffness is computed from the geometry and the material properties of the panel. The limit shear is computed from the largest panel eccentricity attained at the overturning.

$$\frac{1}{K_0} = \frac{12H^3}{cE_M L^3 t} + \frac{H}{G_M L t} \tag{9}$$

Where E_M and G_M are the elastic and shear moduli of the masonry, and c is a coefficient describing the end rotational restraint of the panel, with values in the range {3;12}.

Once $V_{R,sh} < V_{lim}$ is known, the failure displacement can be computed.

3 SHEAR-FLEXURAL FAILURE OF REINFORCED PANELS

The procedure holding for unreinforced masonry panels can be modified in order to include the effect of fiber reinforcement nets added to the external surfaces of the panel. In general, the flexural reinforcement of masonry elements is carried out by adding fiber strips along the vertical edges of the walls or by using fiber cross braces on the wall faces. The shear reinforcement of the panel instead, is best suited by using mortar coatings and fiber meshes on the faces or by using near-surface mounted bars (NSM) resting on the mortar courses.

The flexural reinforcement is based on the introduction of some tensile resisting force that can carry on a bending moment summing up with the one resisted by the masonry alone. On the contrary, shear reinforcement is mainly thought for increasing the shear capacity of the masonry material.

In what follows a reinforced panel is considered, in which the four vertical edges are equipped with unidirectional strips of fibers externally bonded to the bricks (EBR). Moreover, the panel is reinforced in shear by means of two external thin layers of high strength mortar reinforced with glass fiber meshes.

The CNR-UNI documents 200 and 213 [6, 7] contain the basic theoretical formulation for the strength evaluation of fiber reinforcement systems in which the bonding agent is high strength mortar. A homogenization strategy is presented in [1] able to deal with mortar coatings reinforced with fiber meshes.

Considering the panel presented in figure 1 the aim is the definition of a suitable modification for the formulas presented in the previous section.

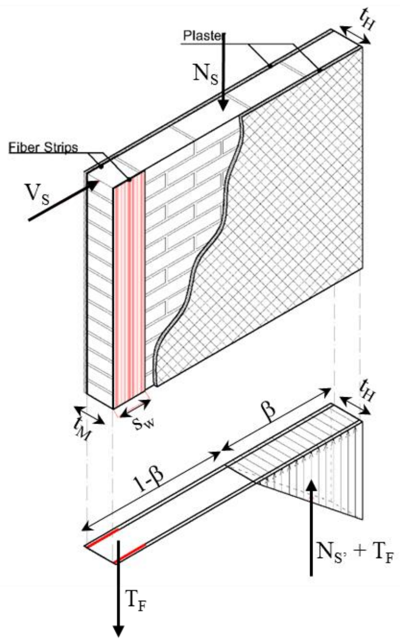

Figure 1: geometry of the considered reinforced panel

By denoting with t_M the thickness of the unreinforced masonry panel, t_L the total thickness of the added reinforcing layers, and with t_H the total thickness of the wall $t_H = t_M + t_L$, it is possible to use the composition rules of series and parallel systems for the calculation of the homogenized shear and compression strength:

$$f_{HV0} = \frac{f_{MV0} t_M + f_{LV0} t_L}{t_M + t_L} \quad , \quad f_{Hc} = \frac{f_{Mc} t_M + f_{Lc} t_L}{t_M + t_L} \tag{10}$$

Where f_{Lc} and f_{LV0} are the compressive and shear strength of the reinforcing coatings. The homogenization through the volumetric ratios is possible if the connection between the masonry panel and the reinforced coatings is sufficiently ductile in leading to the full yielding of both materials.

If the flexural capacity of the panel is not sufficient for the rotational equilibrium, added reinforcement strips on the edges can supply the missing resisting moments. By using formulas for EBR or NSM the axial strength T_F of the reinforcement can be computed:

$$T_F = \sqrt{2 E_F G_F A_F s_w} \tag{11}$$

In formula (10) E_F is the reinforcement elastic modulus, G_F is the fracture energy of the interface, A_F is the reinforcement area and s_w is the breadth of the bonding surface [6].

Once the strength of the flexural reinforcement is defined, the formulas (5, 6) can be modified in order to include the effect of the added strength:

$$\lambda_{\min} = \frac{2D}{2D-1} \frac{(N_S + T_F)}{t_H f_{Hc}} \tag{12.a}$$

$$\bar{\lambda} = \frac{n}{2} \frac{N_S L + 2 T_F d - 2\mu a_V (N_S + T_F)}{N_S + T_F + n a_V t_H f_{HV0}} \tag{12.b}$$

Where d is the distance of the reinforcement axis to the most compressed fiber.
If $\bar{\lambda}$ is larger than $\lambda_{\min}$ the limit shear force is easily computed as:

$$V_{H,sh} = \mu\left(N_S + T_F\right) + \bar{\lambda}\, t_H f_{HV0} \tag{13}$$

Alternately, if $\lambda_{\min}$ is the smallest length, the limit shear force is computed as:

$$V_{H,fl} = \frac{M_{H,fl}}{a_V} = \frac{1}{a_V}\left[N_S \left(\frac{L}{2} - \frac{\lambda_{\min}}{2} \right) + T_F \left(d - \frac{\lambda_{\min}}{2} \right) \right] \tag{14}$$

4 VERIFICATION OF THE PROPOSED FORMULA

The analysis previously defined is applied to a set of eight brick masonry walls tested by Churilov et Al. [8]. The height of the walls was fixed to 1820 mm, while two different lengths respectively equal to 1420 mm and 2820 mm were chosen investigating the effect of the aspect ratio on the lateral capacity of the wall. Since the purpose of the research was the investigation of the in-plane behavior of both unreinforced and jacketed walls, the whole number of specimens was split into two groups, each of which was made of two slender and two squat walls. The walls of only one group were reinforced through the reinforced concrete (RC) jacketing technique.

The reinforcement was applied to the external faces of the panels by executing transversal connection ties over which the steel wire meshes were welded. then two layers of high strength mortar were poured on forms with a thickness of 25 mm approximately.

Table 1 collects the thicknesses t of the masonry components, their elastic modulus E and their tensile and compressive strength, f_t and f_c, respectively. Concerning brick units, the cylindrical compressive strength was computed as 0.83 times the cubic one, while their tensile strength was evaluated from the flexural tensile strength obtained experimentally.

Elastic moduli of mortar and bricks were estimated starting from their compressive strengths [3]. All these properties were used in this paper to compute the mechanical properties of the masonry walls validating the proposed formulas.

The presented experiments considered very squat panels under a very high axial load and repeated alternated increasing displacement cycles. Therefore they constitute a very sharp reference for testing the prediction capability of formulas dealing with shear-compression failure of masonry panels.

Table 1: Geometrical and mechanical properties of the materials.

	t [mm]	f_c [MPa]	f_t [MPa]	E [MPa]
Brick	65	13.6	1.8	6800
Lime Mortar	10	0.6	0.1	300
Concrete	25	22.7	3.6	20000
Steel Wires	Φ 4.2/10	450	450	200000

In Figure 2 some pictures of the failed panels are presented. The cracking pattern shown by the panels highlights a shear sliding failure under high compressive stress with very large contact zones at the two panel ends.

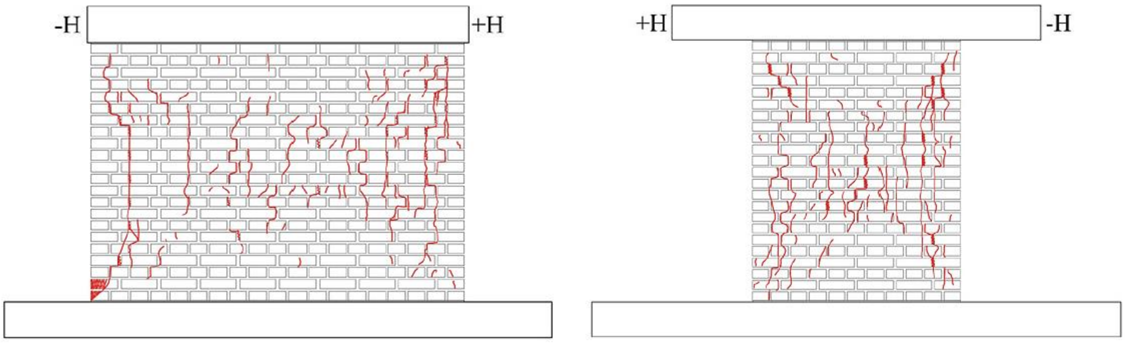

Figure 2: Failure of the panels considered in the Churilov et Al. [8] experimental tests

In what follows the experimental data are compared with the results of the proposed theory in terms of the different possible failure mechanisms, reconstruction of the load-displacement curve and evaluation of the limit displacement at failure. The shear forces V_i are computed through the equations (2.a, 2.b, 2.c) identified by the flexural, the shear, and the crushing-shear failure modes, respectively.

Table 2 presents the comparison of the computed shear forces with the peak forces of the experimental tests of Churilov et Al. [8]. Concerning the displacements, Table 3 collects the maximum displacements δ_{ult} and the percentage drift $\delta_{\%}$ measured in the experimental campaign, compared with the displacements associated with the maximum shear force acting on the wall.

Since the original tests were performed under cyclic loading, two lines described the behavior of the masonry panel along the two opposite directions. For the sake of completeness, both the positive and the negative load-displacement branches were plotted and taken under consideration for the error computation. The maximum analytical displacement $\delta_{V,max}$ provided by the Eq. (8) is the displacement associated with the maximum shear capacity of the wall, assumed as the minimum value among the shears V_1, V_2, V_3 collected in Table 2.

Table 2: Lateral load capacity of URM and SM masonry panels computed for each failure mechanism and under the application of the axial load N.

Units [kN]	URM1	URM2	URM3	URM4	SM1	SM2	SM3	SM4
N	630.00	365.00	315.00	182.50	630.00	365.00	315.00	182.50
V_1	310.22	168.27	179.23	92.12	614.50	311.65	414.61	229.57
V_2	278.72	150.02	157.18	83.02	578.90	288.65	395.41	215.27
V_3	174.14	100.89	139.87	80.96	1056.82	612.28	854.32	494.54
V_{max}	174.14	100.89	139.87	80.96	578.90	288.65	395.41	215.27
V_{exp}	189.14	88.54	157.35	65.46	483.79	227.18	365.15	208.62
$e_{,V}$	9%	-12%	12%	-19%	-16%	-21%	-8%	-3%

Table 3: Experimental [8] and analytical displacements provided for the whole bench of specimens.

Units [mm]	URM1	URM2	URM3	URM4	SM1	SM2	SM3	SM4
δ_{ult}	11.51	16.10	12.86	11.56	12.33	15.05	20.95	21.01
$\delta_{\%}$	0.63	0.88	0.71	0.64	0.68	0.83	1.15	1.15
$\delta_{peak\,+}$	3.87	6.86	8.13	7.02	2.78	8.40	8.44	16.97
$\delta_{peak\,-}$	4.43	7.00	8.35	8.96	3.99	8.93	11.96	15.02
$E\,[\delta_{peak}]$	4.15	6.93	8.24	7.99	3.39	8.67	10.20	16.00
$\delta_{V,max}$	3.10	4.40	5	11.70	20	17.00	17.10	15.4
$e_{,\delta}$	-25%	-37%	-39%	46%	-	96%	68%	-4%

According to what is mentioned before, Figure 3 and Figure 4 illustrate the backbone load-displacement curves of each masonry wall in the two loading directions.

In particular, the solid line describes the lateral capacity of the masonry wall (Eq.8), while red and blue dashed curves are the experimental evolution of the lateral load applied at the top of the wall against the horizontal displacement corresponding to the positive and the negative directions respectively. Two more points are presented in the plots, namely, the triangle identifies the maximum analytical lateral load resisted by the wall, while the circle represents the theoretical maximum displacement given by the existing standards.

The maximum displacements considered by Italian and European standards value are defined as 0.4% and 0.8% of the total height of the panel. Specifically, the first value is associated with the shear-type failure, whereas the other one describes the limit displacement in case of panel overturning.

By observing previous tables and figures, it is very clear that the proposed formula is able to appreciate the maximum value of the lateral load at which the panel fails, even if it is barely accurate only in terms of displacements.

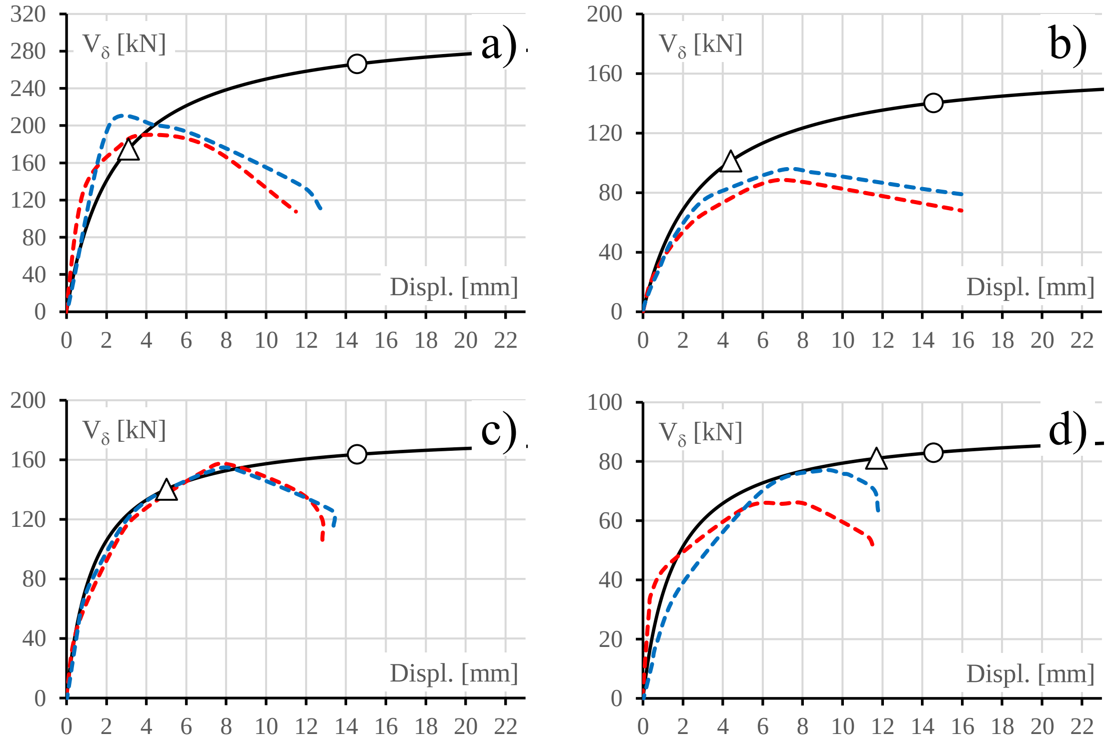

Figure 3: Load-Displacement curves: (a) URM1, (b) URM2, (c) URM3, (d) URM4.

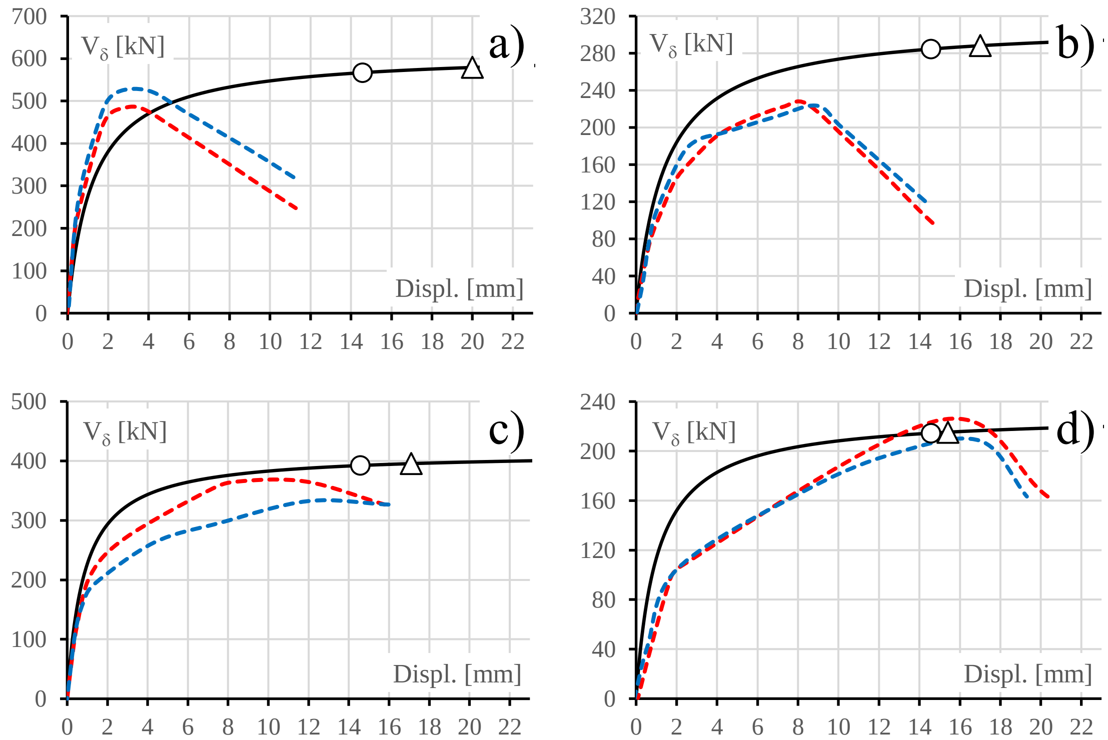

Figure 4: Load-Displacement curves: (a) SM1, (b) SM2, (c) SM3, (d) SM4.

Concerning lateral stiffnesses collected in Table 4, since the hyperbolic curve needs of the value of initial lateral stiffness K_0, its value is computed according to Eq.(9) and it is compared with the value provided experimentally in Churilov et Al [8].

It is to mention that the value of stiffness computed analytically was roughly the double of the secant stiffness obtained experimentally, as previously expected. Consequently, it is extremely important to use the initial stiffness in the load path calculations in order to obtain smaller bias in the estimation of the maximum displacement, as is pointed out by the comparison with the experimental data.

Table 4: Tangential and secant lateral stiffnesses of all the specimens, and their ratio.

Units [kN/mm]	URM1	URM2	URM3	URM4	SM1	SM2	SM3	SM4
K_0	128.93	57.76	128.93	57.76	500.62	224.29	500.62	224.29
K_{exp}	185.610	44.29	74.23	40.30	460.69	102.81	236.28	66.36
ρ_K [-]	0.69	1.30	1.74	1.43	1.09	2.18	2.12	3.38

5 CONCLUSIONS

In the paper, the theoretical framework of the interaction of the failure modes for masonry panels has been discussed in detail. The limit compression zone resulting from the combination of shear and overturning failure has been defined. The shear capacity limitation due to high compression states has been derived in terms of Mohr-Coulomb limit plasticity.

Then, the theoretical framework has been extended to panels reinforced with external coatings of thin FRM layers, and panels reinforced with fiber strips bonded along the vertical edges.

The use of the hyperbolic representation of the load-displacement path allowed the easy construction of the panel' pushover curves. The parameters needed to build the curves were presented and discussed.

By using some experimental results presented in the literature, the effectiveness of the proposed formulation has been demonstrated. The presented results pointed out the importance of considering shear-crushing failure when the axial force has significant value.

The presented procedure is an easy and fast way for the verification and strengthening design of masonry panels subjected to high compression forces, as in monumental buildings.

REFERENCES

[1] Benedetti A. In Plane Behaviour of Masonry Walls Reinforced with Mortar Coatings and Fibre Meshes. *International Journal of Architectural Heritage* (2019) **13**-7:1029-1041, DOI: 10.1080/15583058.2019.1618972

[2] Benedetti A. and Benedetti L. Interaction of shear and flexural collapse modes in the assessment of in-plane capacity of masonry walls. *Proc. of the 12th Canadian Masonry Symposium, Vancouver, Canada, June 2nd -5th, 2013.*

[3] Aprile A, Benedetti A, Grassucci F. 2001. Assessment of Cracking and Collapse for Old Brick Masonry Columns. *Journal of Structural Engineering*, **127**:1427–35. DOI:10.1061/(ASCE)0733-9445(2001)127:12(1427).

[4] Benedetti A, Steli E. Analytical models for shear-displacement curves of unreinforced and FRP reinforced masonry panels. *Construction and Buildings Materials* (2008), **22**(3):175–185. DOI:10.1016/j.conbuildmat.2006.09.005.

[5] Petry S. and Beyer K. Force–displacement response of in-plane-loaded URM walls with a dominating flexural mode, *Earthquake Engng Struct. Dyn.* (2015), DOI: 10.1002/eqe.2597

[6] DT 200-R2. *Guide for the Design and Construction of Externally Bonded FRP Systems for Strengthening Existing Structures*. CNR, Italy (2014).

[7] DT 215. *Istruzioni per la Progettazione, l'Esecuzione ed il Controllo di Interventi di Consolidamento Statico mediante l'utilizzo di Compositi Fibrorinforzati a Matrice Inorganica*. CNR, Italy (2019).

[8] Churilov S., and Dumova-Jovanoska E. In-plane shear behaviour of unreinforced and jacketed brick masonry walls. *Soil Dynamics and Earthquake Engineering* (2013), **50**:85–105. DOI:10.1016/j.soildn.2013.03.006